Int J Clin Exp Med 2019;12(3):2443-2449
www.ijcem.com /ISSN:1940-5901/IJCEM0076695

Original Article

A novel mutation of PITX2 gene in a Chinese family with Axenfeld-Rieger syndrome

Ling Chen[1*], Ming Zhang[2*], Lina Huang[1], Peng Huang[1], Jinci Wan[1]

[1]*Shenzhen Key Laboratory of Ophthalmology, Affiliated Shenzhen Eye Hospital of Jinan University, Shenzhen, Guangdong Province, P. R. China;* [2]*Department of Stomatology, Guangdong Academy of Medical Science & Guangdong General Hospital, Guangzhou, Guangdong Province, P. R. China.* [*]*Equal contributors.*

Received March 25, 2018; Accepted November 9, 2018; Epub March 15, 2019; Published March 30, 2019

Abstract: Axenfeld-Rieger syndrome (ARS) is a rare autosomal dominant disorder characterized by ocular, dental, and other systemic developmental defects. Four genetic loci have been found to be associated with ARS, but no causative gene defect has been found for 40% of the cases of ARS investigated. In this study, the clinical and molecular characteristics of a five-generation Chinese family with ARS were investigated. The pathogenic variant was investigated with specific hereditary eye disease enrichment panels including 369 known genes of inherited ocular disease, based on targeted exome capture technology. The identified variant was confirmed with Sanger sequencing. A novel heterozygous variant c.191C > A (p.P64 Q) in *PITX2* gene was identified to be disease-causing mutation in this pedigree. These results may be useful for better understanding of the spectrum of *PITX2* mutations and the role of *PITX2* in the development and progression of ARS.

Keywords: Axenfeld-Rieger syndrome, PITX2 gene, Chinese family

Introduction

Axenfeld-Rieger syndrome (ARS; OMIM 180-500) is a rare disorder of development, which includes a spectrum of ocular defects and multisystem anomalies. The classic ocular defects of ARS include a posterior embryotoxon, peripheral iridocorneal adhesion, and ultrastructural abnormalities of the trabecular meshwork, iris hypoplasia, corectopia, polycoria, and other less frequent features such as cataracts, microcornea, and retinal detachment. Because of the severe changes in eye structure, approximately half of the individuals affected with ARS develop glaucoma and corneal opacity, which cause severe damage to visual acuity. In addition to the ocular defects, defects in dental development are well-recognized, which include microdontia, anodontia, enamel hypoplasia, misplaced teeth, and maxillary hypoplasia. Other systemic findings can be observed include a redundant periumbilical skin, hearing defects, congenital cardiac or kidney abnormalities. These systemic features are incomplete penetrance and variable expressivity [1-3].

Axenfeld-Rieger syndrome is a genetically developmental disorder and the mode of inheritance is autosomal dominant. Currently, four, genetic loci have been found to be associated with ARS, which include *PITX2* (paired-like homeodomain transcription factor 2; 4q25-q26; OMIM 601542), *FOXC1* (forkhead box C1; 6p25; OMIM 601090), *PAX6* (paired box gene 6; 11p13; OMIM 607108), and a yet to be identified gene at 13q14 (OMIM 601499). For 40% of the cases of Axenfeld-Rieger syndrome investigated, no causative gene defect has been found [1-6].

The clinical and genetic characters in individuals affected with ARS are rarely reported in China [7-10]. The purpose of this study was to investigate the clinical and molecular characteristics of a Chinese family affected by ARS.

Material and methods

Study participants

A five-generation family with Axenfeld-Rieger syndrome from the Guangdong province in

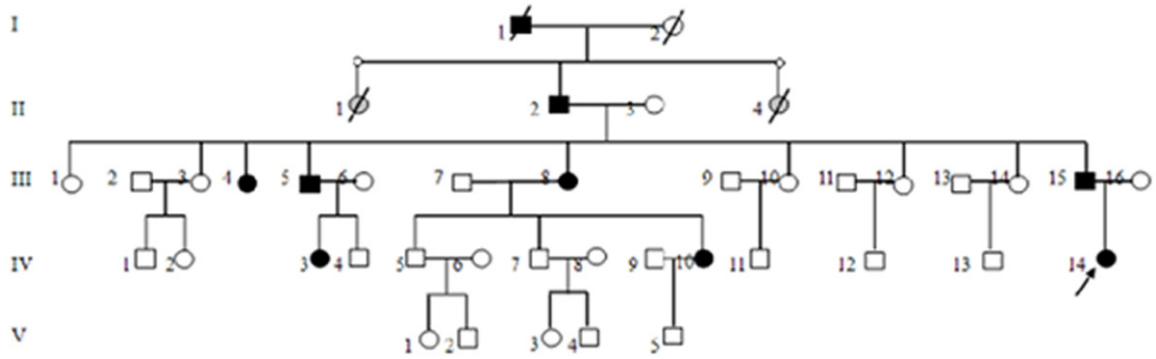

Figure 1. Pedigrees of Axenfeld-Rieger syndrome in this study. Circles represent females and squares represent males. Closed symbols represent affected patients and open symbols indicate unaffected subjects. The proband (IV:14) is indicated with an arrow.

southern part of China was studied (**Figure 1**). Written informed consent was obtained from all subjects, and the study was approved by the Ethics Committees of the Jinan University Affiliated Shenzhen Eye Hospital and conducted in accordance with the Declaration of Helsinki. Ophthalmic examinations by a referring ophthalmologist included corrected visual acuity, slit lamp biomicroscopy, gonioscopy, funduscopy, measurement of intraocular pressure (IOP) by Goldmann applanation tonometer, measurement of corneal diameter and axial length, ocular A scan and B scan. An individual was determined to be affected if multiple of the characteristic ocular findings associated with Axenfeld-Rieger syndrome were observed.

Full examination of dental developmental condition was performed by a dental specialist, including general oromaxillo-facial examination, intraoral examination, panoramic radiography, buccal lateral radiography, and cone beam computed tomography (CBCT).

Other diagnoses were obtained from the patients' attending specialists. Peripheral venous blood samples were obtained from all study participants.

Genetic analysis

DNA library preparation: Each DNA sample was qualified by agarose gel electrophoresis and Nanodrop (Thermo). Libraries were prepared using Illumina standard protocol. Briefly, 3 microgram of genomic DNA was fragmented by nebulization, the fragmented DNA was repaired, an 'A' is ligated to the 3' end, Illumina adapters were then ligated to the fragments, and the sample was size selected aiming for a 350-400 base pair product. The size selected product was then PCR amplified (Each sample is tagged with a unique index during this procedure), and the final product was validated using the Agilent Bioanalyzer.

Targeted genes enrichment and sequencing

The amplified DNA was captured with three ocular-disease related Gene Panels using biotinylated oligo-probes (MyGenostics GenCap Enrichment technologies). The probes were designed to tile along 369 ocular-disease related genes, containing congenital ocular developmental defects, glaucoma, and congenital cataract related genes, including the three known ARS genes (*PITX2, FOXC1,* and *PAX6*). The capture next generation sequencing (CNGS) experiment was conducted according to manufacturer's protocol. In brief, 1 μg DNA library was mixed with Buffer BL and GenCap gene panel probe (MyGenostics, Beijing, China), heated at 95°C for 7 minutes and 65°C for 2 minutes on a PCR thermocycler. Then 23 μl of the 65°C pre-warmed Buffer HY (MyGenostics, Beijing, China) was added to the mix, and the mixture was held at 65°C with the PCR lid heat on for 22 hours for hybridization. Then 50 μl MyOne beads (Life Technology) were washed in 500 μL 1X binding buffer 3 times and resuspended in 80 μl 1X binding buffer. Then 64 μl 2X binding buffer was added to the hybrid mix, and transferred to the tube with 80 μl MyOne beads. The mix was rotated for 1 hour on a rotator. The beads were then washed with WB1 buffer at room temperature for 15 minutes once and WB3 buffer at 65°C for 15 minutes

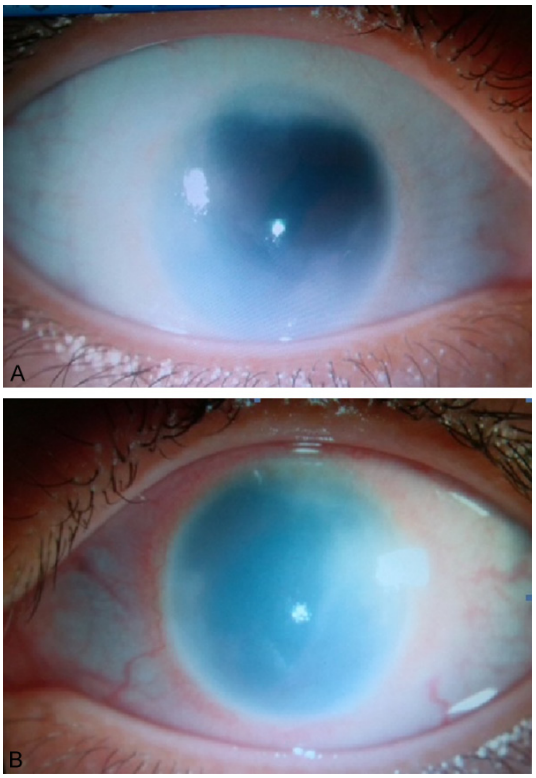

Figure 2. A, B. Clinical examination of ocular anterior segment structure. A. Slit-lamp photograph of opacity in the cornea of right eye in the pro-band (IV:14). B. Slit-lamp photograph of opacity in the cornea of right eye in the pro-band (IV:14).

three times. The bound DNA was then eluted with Buffer Elute. The eluted DNA was finally amplified for 15 cycles using the following program: 98°C for 30 seconds (1 cycle); 98°C for 25 seconds, 65°C for 30 seconds, 72°C for 30 seconds (15 cycles); 72°C for 5 minutes (1 cycle). The PCR product was purified using SPRI beads (Beckman Coulter) according to manufacturer's protocol. The enrichment libraries were sequenced on Illumina HiSeq 2000 sequencer for paired read 100 bp [11, 12].

Bioinformatics analysis

After HiSeq 2000 sequencing, high-quality reads were retrieved from raw reads by filtering out the low quality reads and adaptor sequences using the Solexa QA package and the cutadapt program (http://code.google.com/p/cutadapt/), respectively. SOAPaligner program was then used to align the clean read sequences to the human reference genome (hg 19). After the PCR duplicates were removed by the Picard software, the SNPs was identified using the SOAPsnp program (http://soap.genomics.org.cn/soapsnp.html). Subsequently, the reads were realigned to the reference genome using BWA and identified the insertions or deletions (InDels) using the GATK program (http://www.broadinstitute.org/gsa/wiki/index.php/Home_Page). The identified SNPs and InDels were annotated using the Exome-assistant program (http://122.228.158.106/exomeassistant). MagicViewer was used to view the short read alignment and validate the candidate SNPs and InDels. Nonsynonymous variants were evaluated by four algorithms, Ployphen, SIFT, PANTHER, and Pmut, as described previously to determine pathogenicity [11, 12].

Expanded validation

DNA samples of all the family members were taken for the same targeted exome sequencing and filtering strategy. To validate all likely pathogenic variants, conventional Sanger sequencing was performed on all the affected and unaffected subjects, and to perform familial segregation analyses whenever possible. Purified PCR products were cycle-sequenced on an ABI 3500 Genetic Analyzer (Applied Biosystems, CA). The results of Sanger sequencing were analyzed by Mutation Surveyor (Softgenetics, PA).

Results

Clinical findings

The proband (IV:14) was a 19 year-old girl who had experienced defective vision since childhood. Her corrected visual acuity was 20/100 in the right eye and hand moving in the left eye. Ocular examination displayed opacity in the peripheral part of the cornea, closure of the anterior chamber angle, glaucomatous atrophy of the optic nerve one the right eye, and opacity in the total part of the cornea and prevented examination of the lens and ocular fundus on the left eye (**Figure 2A**, **2B**). The IOPs were 32 mmHg on the right eye and 22 mmHg on the left eye. The axial lengths were 25.47 mm on the right eye and 30.10 mm on the left eye. The diameters of the cornea were 10 mm on the both eyes. Ocular B scan showed no detachment of the retina on both eyes.

Dental examination displayed multiple dentition defects, porcelain bridge repair of lost anterior teeth, dental caries, residual roots,

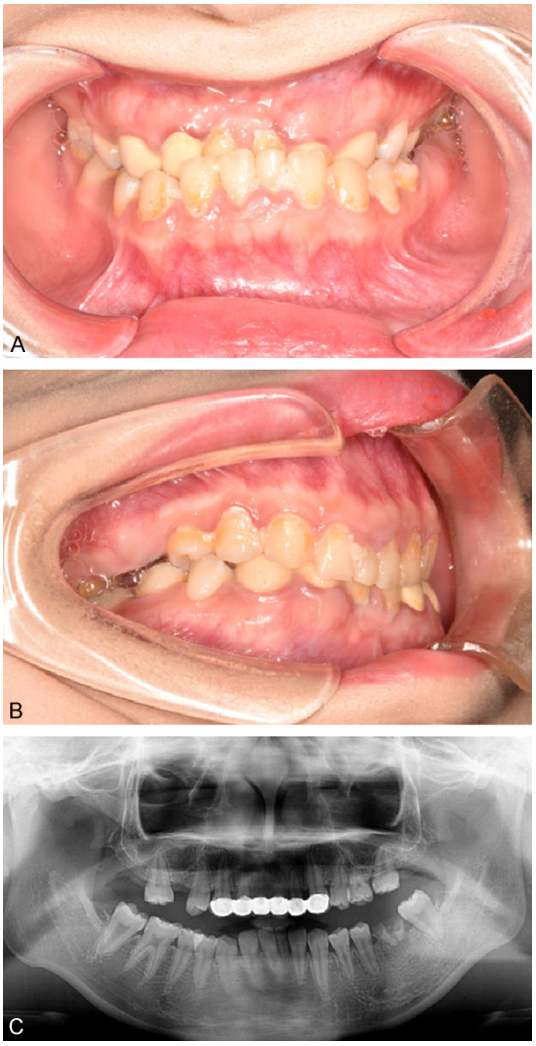

Figure 3. A-C. Examinations revealed dental anomalies. Dental examination displayed multiple dentition defects, porcelain bridge repair of lost anterior teeth, dental caries, residual roots, retained deciduous teeth.

and retained deciduous teeth (**Figure 3A-C**). The other nonocular abnormalities of the proband consisted of redundant periumbilical skin (**Figure 4**). She had no cardiac, kidney or hearing defect.

The other affected individuals I:1, II:2, III:4, III:5, III:8, III:15, IV:3, IV:10 all had similar positive signs as with the proband, except that individual IV:3 hadn't the ocular and dental abnormality.

Mutation analysis

The capture next generation sequencing (CNGS) results were then calculated for quality.

Figure 4. Photograph of the redundant periumbilical skin.

The average sequencing depths and coverage of the target regions were 200 reads and more than 98.0%, respectively. After processing of raw data through the BWA program, variants were called and annotated using GATK. Numerous non-synonymous variants were identified by the GATK program. The mutations identified were searched in multiple databases, including the 1000 Genome (1000G, http://www.1000genomes.org/), ESP6500 (http://evs.gs.washington.edu/EVS/) and 702 sample in-house exome database as normal controls. The candidate mutations were not present or present at extremely low frequency in these databases. Any variants that were reported in the HapMap 28 and the SNP release of the 1000 Genome Project with a MAF > 0.05 were removed. To evaluate the pathogenicity of the variants, bioinformatics tools were used to analyze potential impacts on the function or structure of the encoded proteins. By employing this stepwise analyses approach, a list of 30 selected candidate variants were obtained for the proband. Finally, there was only one heterozygous variant in *PITX2* gene was identified as the potential disease-causing mutation in the pedigree. Sanger sequencing validation and segregation analysis were then performed, which demonstrated that the heterozygous variant c.191C > A (p.P64 Q) in *PITX2* gene was disease-causing mutation in this pedigree (**Figure 5A**, **5B**).

Discussion

Axenfeld-Rieger syndrome is known to be associated with four genetic loci, which include *PITX2, FOXC1,* and *PAX6* gene. Additionally, 40% of the cases of ARS investigated haven't

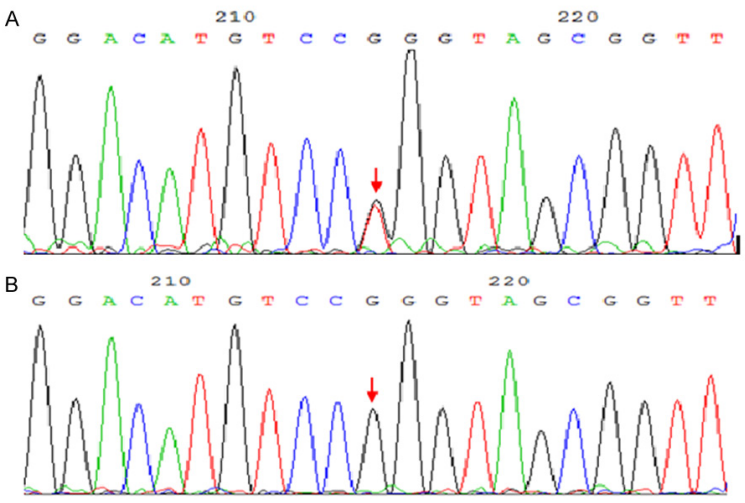

Figure 5. A, B. Partial nucleotide sequence of *PITX2* gene. A. The sequence in an affected subject shows a heterozygous G > T transversion (indicated by the arrow). The nucleotide substitution at codon 64 results in a change from proline to glutamine. B. Unaffected family members and the general population lack this nucleotide change.

been found causative gene defect. ARS is characterized by complete penetrance, but disease severity shows variability. There was no obvious correlation between the gene defect and the severity of the phenotype. But there was a trend to be observed that ARS patients who display defects in anterior segment abnormalities (anterior segment dysgenesis, ASD) of the eye and other organ systems had mutations of the *PITX2* gene. Additionally, in patients with isolated ASD, mainly *FOXC1* mutations were detected [1-7, 13-15]. In this study, a mutation c.191C > A (p.P64 Q) in *PITX2* gene in a southern Chinese pedigree with ARS was detected. Full-spectrum ARS including ocular abnormalities: opacity in the cornea, closure of the anterior chamber angle, atrophy of the optic nerve, increased IOP; dental defects: multiple dentition defects, loss of anterior teeth, dental caries, residual roots, retained deciduous teeth, and redundant periumbilical skin were found in affected individuals in this pedigree. This result was consistent with those of previous studies showing that ARS patient who display defects in ASD of the eye and other organ systems had mutations of the *PITX2* gene.

The *PITX2* gene encodes a homeodomain-containing developmental transcription factor which regulates expression of downstream target genes through binding to specific DNA sequences and activating transcription, playing an important role in orchestrating normal embryonic development. *PITX2* is expressed very early during tooth development. From experimental data it seems likely that the molecular basis of tooth anomalies in ARS is the inability of mutant *PITX2* to activate *DLX2* gene which is required for tooth and craniofacial development, and it has been shown that expression of *PITX2* in the neural crest is also necessary for optic stalk and anterior segment structure development [1-7, 14-18].

PITX2 is a 60 amino acid homeodomain protein with a lysine at residue 50 that is characteristic of the bicoid-related proteins. The homeodomain is responsible for recognizing specific DNA sequences to bring the transcription factors to proper target genes. This 60 amino acid domain is composed of three helices and a flexible NH2-terminal arm. Its integrity is essential for binding DNA and is critical for PITX2 to act as a transcription factor. To date, 104 mutations of the *PITX2* gene have been associated with ARS and other cases of anterior segment malformations, such as iridogoniodysgenesis, iris hypoplasia, and Peters' anomaly [1-7, 19-21]. Except a few intronic mutations, most of the mutations detected in human *PITX2* are point mutations in the homeodomain or COOH-terminal domains (The Human Gene Mutation Database, HGMD). In this study, a novel mutation, c.191C > A (p.P64Q) point mutation, changing proline to glutamine in codon 64 of the protein was found in a southern Chinese family with ARS.

The mutations in this position, missense mutations P64L and P64R have been reported before in pedigrees with ARS, but this particular change P64Q has not been reported yet. Experimental data show that mutant PITX2 proteins that harbor missense mutations in their homeodomain demonstrated reduced or even abolished DNA binding. Amino acid position 64 is located in the loop between helices 1 and 2 of the homeodomain and is conserved considerably between homeodo-

main-containing proteins. Because of the rigid structure, proline residues provoke the orientation of helices and are therefore often found in loops. It may be that a replacement of this proline residue with leucine, arginine, or glutamine changes the orientation of the first and third helices and subsequently alters the stability of the homeodomain [15, 22, 23]. In summary, this is a report of a novel mutation P64Q in *PITX2*, which expands our knowledge of the role of *PITX2* in genetic causes of ARS.

Acknowledgements

This study was supported by grants from the Basic Research Program of Science and Innovation Commission Foundation of Shenzhen City, China (JCYJ20140414114853651), Medical Scientific Research Foundation of Guangdong Province, China (A2014641) and by the Shenzhen Science and Technology Project (201302132). The authors are thankful to the participants for their participation in the study.

Disclosure of conflict of interest

None.

Address correspondence to: Ling Chen, Shenzhen Key Laboratory of Ophthalmology, Shenzhen Eye Hospital, Affiliated Shenzhen Eye Hospital of Jinan University, Room No. 245, No. 18 Zetian Road, Futian District, Shenzhen 518040, Guangdong Province, P. R. China. Tel: 0086-0755-23959600; 008618925257378; E-mail: asdf07910010@163.com; Ming Zhang, Department of Stomatology, Guangdong Academy of Medical Science & Guangdong General Hospital, No. 106, 2nd Yat-*Sen Road, Yuexiu District, Guangzhou 510080, Guangdong Province, P. R. China. Tel: 0086-02083882222; E-mail: zhangm882@163.com

References

[1] Amendt BA, Semina EV, Alward WL. Rieger syndrome: a clinical, molecular, and biochemical analysis. Cell Mol Life Sci 2000; 57: 1652-66.
[2] Seifi M, Walter MA. Axenfeld-Rieger syndrome. Clin Genet 2018; 93: 1123-1130.
[3] Tumer Z, Bach-Holm D. Axenfeld-Rieger syndrome and spectrum of PITX2 and FOXC1 mutations. Eur J Hum Genet 2009; 17: 1527-39.
[4] Alward WL. Axenfeld-Rieger syndrome in the age of molecular genetics. Am J Ophthalmol 2000; 130: 107-15.
[5] Fuse N, Takahashi K, Yokokura S, Nishida K. Novel mutations in the FOXC1 gene in Japanese patients with Axenfeld-Rieger syndrome. Mol Vis 2007; 13: 1005-9.
[6] Kim GN, Ki CS, Seo SW, Yoo JM, Han YS, Chung IY, Park JM, Kim SJ. A novel forkhead box C1 gene mutation in a korean family with Axenfeld-Rieger syndrome. Mol Vis 2013; 19: 935-43.
[7] Li DD, Zhu QG, Lin H, Zhou N, Qi YH. A novel PITX2 mutation in a Chinese family with Axenfeld-Rieger syndrome. Mol Vis 2008; 14: 2205-10.
[8] Peng XX, Mao WS, Ye TC. [Axenfeld-Rieger syndrome-a report of 10 cases]. Yan Ke Xue Bao 1987; 3: 244-7.
[9] Yin HF, Fang XY, Jin CF, Yin JF, Li JY, Zhao SJ, Miao Q, Song FW. Identification of a novel frameshift mutation in PITX2 gene in a chinese family with Axenfeld-Rieger syndrome. J Zhejiang Univ Sci B 2014; 15: 43-50.
[10] Wang Y, Zhao H, Zhang X, Feng H. Novel identification of a four-base-pair deletion mutation in PITX2 in a Rieger syndrome family. J Dent Res 2003; 82: 1008-12.
[11] Huang XF, Xiang P, Chen J, Xing DJ, Huang N, Min QJ, Gu F, Tong Y, Pang CP, Qu J, Jing ZB. Targeted exome sequencing identified novel USH2A mutations in Usher syndrome families. PLoS One 2013; 8: e63832.
[12] Shu HR, Bi H, Pan YC, Xu HY, Song JX, Hu J. Targeted exome sequencing reveals novel USH2A mutations in chinese patients with simplex Usher syndrome. BMC Med Genet 2015; 16: 83.
[13] Gripp KW, Hopkins E, Jenny K, Thacker D, Salvin J. Cardiac anomalies in Axenfeld-Rieger syndrome due to a novel FOXC1 mutation. Am J Med Genet A 2013; 161A: 114-9.
[14] Zhao CM, Peng LY, Li L, Liu XY, Wang J, Zhang XL, Yuan F, Li RG, Qiu XB, Yang YQ. PITX2 loss-of-function mutation contributes to congenital endocardial cushion defect and Axenfeld-Rieger syndrome. PLoS One 2015; 10: e0124409.
[15] Dressler S, Meyer-Marcotty P, Weisschuh N, Momeni AJ, Pieper K, Gramer G, Gramer E. Dental and craniofacial anomalies associated with Axenfeld-Rieger syndrome with PITX2 mutation. Case Rep Med 2010; 2010: 621984.
[16] Chen L, Gage PJ. Heterozygous pitx2 null mice accurately recapitulate the ocular features of Axenfeld-Rieger syndrome and congenital glaucoma. Invest Ophthalmol Vis Sci 2016; 57: 5023-30.
[17] Li X, Venugopalan SR, Cao HJ, Pinho FO, Paine ML, Snead ML, Semina EV, Amendt BA. A model for the molecular underpinnings of tooth defects in Axenfeld-Rieger syndrome. Hum Mol Genet 2014; 23: 194-208.

[18] Volkmann BA, Zinkevich NS, Mustonen A, Scbilter KF, Bosenko DV, Rais LM, Broeckel U, Link BA, Semina EV. Potential novel mechanism for Axenfeld-Rieger syndrome: deletion of a distant region containing regulatory elements of PITX2. Invest Ophthalmol Vis Sci 2011; 52: 1450-9.

[19] Holmberg J, Liu CY, Hjalt TA. PITX2 gain-of-function in Rieger syndrome eye model. Am J Pathol 2004; 165: 1633-41.

[20] Doward W, Perveen R, Lloyd IC, Ridgway AEA, Wilson L, Black GC. A mutation in the RIEG1 gene associated with Peters' anomaly. J Med Genet 1999; 36: 152-5.

[21] Kulak SC, Kozlowski K, Semina EV, Pearce WG, Walter MA. Mutation in the RIEG1 gene in patients with iridogoniodysgenesis syndrome. Hum Mol Genet 1998; 7: 1113-7.

[22] Phillips JC. Four novel mutations in the PITX2 gene in patients with Axenfeld-Rieger syndrome. Ophthalmic Res 2002; 34: 324-6.

[23] Weisschuh N, Dressler P, Schuettauf F, Wolf C, Wissinger B, Gramer E. Novel mutations of FOXC1 and PITX2 in patients with Axenfeld-Rieger malformations. Invest Ophthalmol Vis Sci 2006; 47: 3846-52.